Ab Initio Studies of Decarboxylations of the β-Keto Carboxylic Acids $XCOCH_2COOH$ (X = H, OH, and CH_3)

Chun-Liang Huang, Chen-Chang Wu, and Min-Hsiung Lien*

Department of Chemistry, National Chung Hsing University, Taichung 402, Taiwan, R.O.C.

Received: April 11, 1997; In Final Form: July 14, 1997[⊗]

Ab initio molecular orbital theory has been used to investigate the gas phase decarboxylations of the β-keto carboxylic acids $XCOCH_2COOH$ (X = H, OH, and CH_3). Structures for stationary points representing reactants, transition states, and products on the potential energy surface have been optimized and characterized at the MP2(Full)/6-31G* level of theory. Based on these, the single-point calculations were performed at the MP4SDTQ(FC)/6-311++G**//MP2(Full)/6-31G** level of theory. The reaction pathways connecting the transition structures and the corresponding equilibrium structures were followed by the intrinsic reaction coordinate (IRC) procedure. For each decarboxylation, channels via the four- and six-membered ring transition structures were both considered. In all cases, the latter are found to be energetically favored over the former. The predicted decarboxylation barriers in the gas phase are 23.8, 23.3, and 28.5 kcal/mol for 3-oxopropanoic acid, acetoacetic acid, and malonic acid, respectively. The computed value of 28.5 kcal/mol is in good agreement with the corresponding experimental results of malonic acid obtained in solutions of various solvents. Self-consistent reaction field (SCRF) calculations based on Onsager's solvent cavity model were performed to assess the solvent effect on the changes in the geometries of the reactants and transition structures. The energy barriers in going from the gas phase to the medium were also explored. Results show that the changes are marginal. No experimental data of decarboxylation are available for 3-oxopropanoic acid and acetoacetic acid for comparison. Using the computed relative energies, moment of inertia, and vibrational frequencies, transition state theory (TST) rate constants were calculated for the decarboxylations in the gas phase.

Introduction

Decarboxylation of carboxylic acids require demanding conditions such as strong base and high temperatures. For example, the prototype carboxylic acid, formic acid (HCOOH), was reported to decarboxylate at 457−780 °C.[1] Early ab initio calculations in 1986[2] and 1987[3] by Ruelle et al. predicted its barrier to decarboxylation to be 77.6 kcal/mol (MP2/6-31G**//HF/6-31G*) and 76.0 kcal/mol (MP4SDTQ/6-31G**//MP2/6-31G**) respectively. Recent studies of Francisco[4] and Schaefer[5] at higher levels of theory led to the lower energy barriers of 65.2 kcal/mol (PMP4/6-311G**//UMP2/6-311G**) and 71.0 kcal/mol (CCSDT-1/DZ+P) in 1992. Bamford and Dewar[6] observed in 1949 that the decarboxylation of acetic acid (CH_3-COOH) was also a high-temperature (770−920 °C) process with a barrier of 67.5 kcal/mol. Later experimental methods such as static system, flow system, and single-pulse shock tube were used to obtain the barriers of 58.5 kcal/mol (at 460−595 °C) and 69.8 kcal/mol (above 700 °C) and 72.9 kcal/mol (at 1300−1950 K) in 1968, 1969, and 1984 by Blake et al.,[7] Blake et al.,[8] and Mackie et al.,[9] respectively. There had been numerous theoretical reports on the decarboxylation of acetic acid before the most recent G-2 calculations of Page et al.[10] and QCISD-(TC) calculations of Nguyen et al.[11] in 1995. Both of them predicted an energy barrier of 72.0 kcal/mol for the thermal process. By contrast, keto carboxylic acids are characterized by their ready thermal decarboxylation. For example, the decarboxylations of the α-keto carboxylic acids (XCOCOOH) glyoxylic acid (X = H), pyruvic acid (X = CH_3), and oxalic acid (X = OH) occur with respective energy barriers (the theoretical predictions in parentheses) of 30.8[12] (45.2[13]), 27.7[14] and 40.0[15] (30.5[16] and 40.8[15]), and 30.0[17] (36.6[18]) kcal/mol. Concerning the decarboxylations of β-keto carboxylic acids,

CHART 1

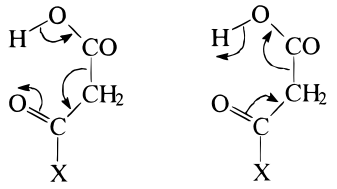

Pollak et al. reported the first experimental investigation of the loss of carbon dioxide from the β-keto carboxylic acids in 1907.[19] Since then, numerous studies have been devoted to the amine-catalyzed decarboxylation of these acids.[20] Ljunggren[21] noted in 1925 that primary amines were better catalysts than the secondary and tertiary amines in facilitating the removal of CO_2. In the absence of amines and other catalysts, Pedersen[22] observed some derivatives of acetoacetic acid and malonic acid to undergo decarboxylation at room temperature. Swain et al.[23] and Bigleg et al.[24] investigated the isotope effect and the IR spectra of these systems and proposed a mechanism in which the decarboxylation takes place via a proton transfer rather than a hydride shift (Chart 1). Westheimer and Jones,[25] Esteve,[26] and Bigley and Thurman[27] explored the effect of solvents of various compositions. They reported that the dielectric constants of the solvents had little effect on the rates of the unimolecular decarboxylations. These experimental observations suggest that ab initio calculations can also be applied to the condensed-phase systems such as that of the β-keto carboxylic acids in which unimolecular thermal decomposition occurs with minimal solvent effect. We are unaware of any theoretical studies on the decarboxylation of these β-keto carboxylic acids, while malonic acid (X = OH) has been observed to decarboxylate with the barriers ranging from 26.9−33.0[28] kcal/mol in liquid phase. In this study we present ab initio molecular orbital

[⊗] Abstract published in *Advance ACS Abstracts,* September 15, 1997.

S1089-5639(97)01266-8 CCC: $14.00

calculations on the decarboxylations of the β-keto carboxylic acids $XCOCH_2COOH$ (X = H, CH_3, and OH).

Computational Method

Ab initio molecular orbital calculations were carried out with the Gaussian 92[29] series of programs. Geometric structures were fully optimized at both MP2(Full)[30]/6-31G*[31] and HF/6-31G* levels of theory. Harmonic vibrational frequencies were calculated at the same level of the theory in order to characterize the stationary points as local minima (equilibrium structures) or first-order saddle points (transition structures) on the potential energy surface (PES) and to evaluate the zero-point vibrational energy (ZPVE). Since the computed harmonic vibrational frequencies overestimate the experimental fundamental frequencies, the ZPVEs were scaled by the respective correction factors of 0.89[32] and 0.9[33] for the Hartree−Fock and MP2 levels of theory. To further correct for electron correlation, single-point calculations were carried out at the MP4SDTQ(FC)/6-311++G**//MP2(Full)/6-31G** level of theory. The natural bond orbital (NBO)[34] technique was applied to calculate the bond order and natural population analysis (NPA). To establish the connection between the transition structures and corresponding equilibrium structures, the reaction pathways were followed using the intrinsic reaction coordinate (IRC)[35] procedure. To account for the effect of the medium, the SCRF calculations based on the Onsager's cavity model[36] of electrostatic solvation were performed for all the species considered in this study. All structures were optimized at the HF/6-31G* level of theory with $\epsilon = 1.0$ (corresponding to the gas phase). Similarly $\epsilon = 4.22$ (simulating the solvent phenetole) and $\epsilon = 34.78$ (for the polar solvent, nitrobenzene), followed by the usual frequency calculations for the structural characterizations. Using these HF/6-31G* geometries, single-point calculations at the MP2(Full)/6-31G* level were carried out to obtain the improved relative energies. 0.5 Å was added to the computed cavity radius (a_0) from the molar volume in order to account for the van der Waals effect of the nearest solvent molecules. TST rate constants for the decarboxylation were computed from the ab initio relative energies, moment of inertia, and vibrational frequencies. All computations were performed on an IBM RS/6000 computer and a C3840 CONVEX supercomputer.

Results and Discussion

Figure 1 shows the geometries optimized at various levels of theory for the reactants, transition states, and products of the β-keto carboxylic acids in this study. **1**, **3**, **5**, **7**, **9**, **12**, **14**, and **16** depict the equilibrium structures whereas **2**, **4**, **6**, **8**, **10**, **11**, **13**, **15**, and **17** present the transition structures on the reaction paths. The complete set of optimal geometric parameters of all stationary points (in Cartesian coordinate), the bond orders, and the population analyses are all available in the Supporting Information. (See Supporting Information paragraph at the end of the text.) Since the relative energies and energy barriers to rotation among the conformers are relatively small and do not significantly affect any mechanistic considerations, we will consider only those conformers which are most directly relevant to the transition structures as precursors on the reaction path. For each decarboxylation, channels involving the four- and six-membered ring transition structures were both considered. In all cases, the latter is found to be the lower energy process. Pathways (1)−(3) involve six-membered ring transition states in which the oxygen of the β-keto group acts as a proton acceptor toward the oxygen of the hydroxyl group thus forming the enol form of the remaining carboxylic acid or ketone. A subsequent 1,3 hydrogen shift yields the more stable carboxylic or keto form.

$$\mathbf{1} \rightarrow \mathbf{2} \rightarrow \mathbf{3} + CO_2 \rightarrow \mathbf{4} + CO_2 \rightarrow \text{acetaldehyde} + CO_2 \quad (1)$$

$$\mathbf{7} \rightarrow \mathbf{8} \rightarrow \mathbf{9} + CO_2 \rightarrow \mathbf{10} + CO_2 \rightarrow \text{acetone} + CO_2 \quad (2)$$

$$\mathbf{12} \rightarrow \mathbf{13} \rightarrow \mathbf{14} + CO_2 \rightarrow \mathbf{15} + CO_2 \rightarrow \text{acetic acid} + CO_2 \quad (3)$$

The less favorable pathways, (4)−(6), all lead to a four-membered ring transition structure.

$$\mathbf{5} \rightarrow \mathbf{6} \rightarrow \text{acetaldehyde} + CO_2 \quad (4)$$

$$\mathbf{7} \rightarrow \mathbf{11} \rightarrow \text{acetone} + CO_2 \quad (5)$$

$$\mathbf{16} \rightarrow \mathbf{17} \rightarrow \text{acetic acid} + CO_2 \quad (6)$$

Unless otherwise noted, only the results from the MP2(Full)/6-31G* calculations will be discussed in the text.

1. Geometric Structures. The six-membered ring transition structures in (1)−(3) resemble those of the McLafferty rearrangement. Brun and Waegall[37] have noted that the rate of this rearrangement becomes slow if the distance between the migrating hydrogen and the accepting carbonyl oxygen is greater than 2.1 Å. In this study, the corresponding distances in **1**, **7**, and **12** are all shorter than 2.1 Å. The precursors in (1)−(3) are therefore predicted to readily undergo hydrogen migrations and then decarboxylations in a concerted fashion. Figure 1 also shows that the migrating hydrogens lie closer to the carbonyl oxygens than to the carboxy oxygens in the transition structures (**2**, **8**, and **13**). They are very close to the length of an O−H single bond (∼0.98 Å). This indicates that the hydrogen shift from carboxyl oxygen to carbonyl oxygen is nearly completed in the transition structures. The observation is further supported by the calculated bond orders between the corresponding atoms during the course of the hydrogen shift as the bond orders between the migrating hydrogen and carbonyl oxygen in the six-membered transition structures **2**, **8**, and **13** are roughly 0.6. These are comparable to those of 0.7 between the migrating hydrogen and the oxygen in the enol forms (**3**, **9**, and **14**). On going from the carboxylic acids to the transition states, the bond orders of the breaking C−C single bonds decrease by about 0.4 while the corresponding forming O−H bonds increase by approximately 0.5. In contrast to those in (1)−(3), the migrating hydrogens in (4)−(6) are closer to the carboxyl oxygen in the transition structures (**6**, **11**, and **17**). The cleaving C−C bonds in these four-membered ring transition structures all have large bond distances (>1.96 Å) and drastically reduced bond orders. The Mulliken population analysis and natural population analysis show that the migrating hydrogens in the reactants and transition states all carry more than 0.5 positive charge in (1)−(3) and that the latter are always more positive than the former is indicative of proton-transfer processes in the decarboxylation of β-keto carboxylic acids.

2. Relative Energies and Barriers to Decarboxylations in the Gas Phase. The schematic potential energy surfaces for the decarboxylation of 3-oxopropanoic acid, acetoacetic acid, and malonic acid are depicted in Figures 2, 3, and 4, respectively; in Table 1 the corresponding total energies and relative energies are listed. Due to the strain energies, the four-membered ring transition structures are less stable than those of the six-membered ring structures by 35.7−63.5 kcal/mol at the MP2(Full)/6-31G* level. Therefore, the former require larger activation energies than the later. The barriers to decarboxylations in (1)−(3) are 23.8 (26.3), 23.3 (25.7), and

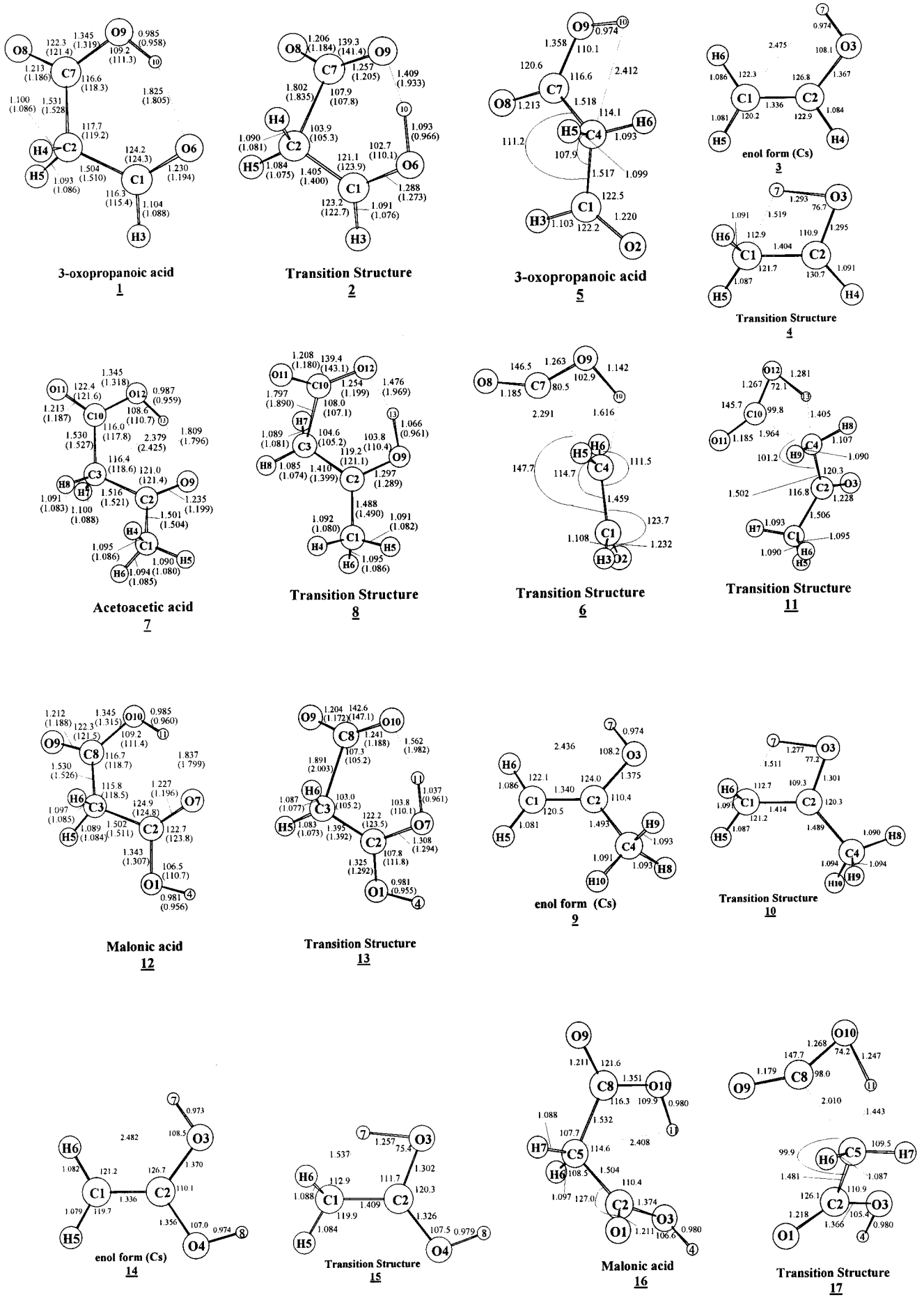

Figure 1. Geometric parameters (MP2(Full)/6-31G* and SCRF $\epsilon = 34.78$ (in parentheses)).

TABLE 1: Total Energies (hartrees), ZPE (kcal/mol), and Relative Energies (kcal/mol)

	HF			MP2			MP4	
molecular	total energy	ZPE[a]	ΔE[b]	total energy	ZPE[c]	ΔE[b]	total energy	ΔE[g]
1	−340.523 57	43.6	0.0	−341.453 12	41.3	0.0	−341.704 15	0.0
1[d]	−340.528 08	43.7	0.0	−341.451 31	43.7[f]	0.0		
1[e]	−340.530 24	43.7	0.0	−341.453 28	43.7[f]	0.0		
2	−340.459 10	42.2	39.0	−341.407 78	39.2	26.3	−341.662 57	23.8
2[d]	−340.466 17	42.3	37.5	−341.406 10	42.3[f]	27.0		
2[e]	−340.469 27	42.3	36.8	−341.408 53	42.3[f]	26.7		
5	−340.517 57	43.2	3.3	−341.444 45	40.8	4.9		
6	−340.328 45	39.5	118.3	−341.295 50	37.1	94.7		
3	−152.888 89	34.1		−153.332 16	32.4			
4	−152.770 82	30.3		−153.237 71	29.1			
CH_3CHO	−152.915 97	33.5		−153.358 97	32.2			
7	−379.571 98	60.4	0.0	−380.637 93	57.7	0.0	−380.931 26	0.0
7[d]	−379.576 37	60.4	0.0	−380.636 15	60.4[f]	0.0		
7[e]	−379.578 50	60.4	0.0	−380.638 10	60.4[f]	0.0		
8	−379.510 63	58.7	36.8	−380.593 58	55.6	25.7	−380.890 30	23.3
8[d]	−379.517 57	58.7	35.2	−380.593 31	58.7[f]	25.2		
8[e]	−379.520 52	58.6	34.7	−380.595 71	58.6[f]	24.9		
11	−379.420 22	54.9	89.7	−380.518 63	52.6	69.8		
9	−191.932 34	50.9		−192.511 65	48.8			
10	−191.820 52	46.9		−192.421 37	45.4			
$(CH_3)_2CO$	−191.962 24	50.2		−192.540 87	48.6			
12	−415.417 90	47.3	0.0	−416.527 73	44.7	0.0	−416.828 41	0.0
12[d]	−415.422 94	47.2	0.0	−416.525 44	47.2[f]	0.0		
12[e]	−415.425 43	47.2	0.0	−416.527 89	47.2[f]	0.0		
13	−415.348 60	45.4	41.6	−416.475 12	42.7	31.0	-416.779 37	28.5
13[d]	−415.354 27	45.2	41.1	−416.471 05	45.2[f]	32.1		
13[e]	−415.356 77	45.1	40.9	−416.472 55	45.1[f]	32.6		
16	−415.412 07	47.3	3.6	−416.523 45	44.5	2.5		
17	−415.267 78	42.0	88.8	−416.409 30	39.6	69.3		
14	−227.754 19	36.8		−228.375 80	34.6			
15	−227.659 67	33.9		−228.301 97	32.4			
CH_3COOH	−227.810 65	37.4		−228.433 98	35.7			
CO_2	−187.634 18	7.1		−188.118 36	6.5			

[a] Scaled by 0.89. [b] Relative energy to the total energies of the respective β-keto carboxylic acids. [c] Scale by 0.9. [d] SCRF calculation ($\epsilon = 4.22$). [e] SCRF calculation ($\epsilon = 34.78$). [f] Thermal energies at the HF/6-31G* level used. [g] Thermal energies at the MP2/6-31G** level used.

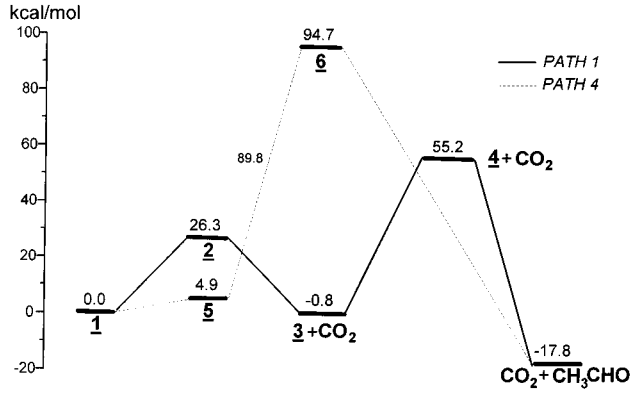

Figure 2. Energy profile for the unimolecular pyrolysis of 3-oxopropanoic acid (MP2/6-31G*//MP2/6-31G*).

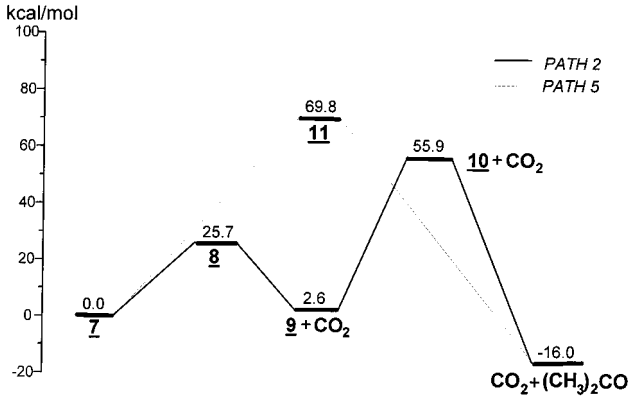

Figure 3. Energy profile for the unimolecular pyrolysis of acetoacetic acid (MP2/6-31G*//MP2/6-31G*).

28.5 (31.0) kcal/mol at the MP4SDTQ(FC)/6-311++G** level and MP2(Full)/6-31G* (in parentheses) as compared with those of 89.8, 69.8, and 66.7 kcal/mol at the MP2(Full)/6-31G* level obtained in (4)−(6) for 3-oxopropanoic acid, acetoacetic acid, and malonic acid, respectively. On the basis of the results we would predict that the β-keto carboxylic acids decarboxylate via the relatively lower energy pathways of the six-membered ring transition structures. This is generally in agreement with the experimental results of Schenkel et al. and Cantwell et al.[38] who have reported that β-keto carboxylic acids undergo the decarboxylations at temperatures around 373 K. Table 2 compares the theoretical results of this study and experimental data. It is seen that the MP4 gas phase decarboxylation barrier of 28.5 kcal/mol for malonic acid is close to those of Clark's observations in solutions of the solvents of phenetole, nitrobenzene, β-chlorophenetole, *p*-dimethoxybenzene, and aniline. This predicted gas phase data is also in good agreement with the experimental data in the liquid phase. This illustrates that the polarity of a solvent has little effect on the activation energy in the decarboxylation. At present no experimental data are available for the decarboxylations of 3-oxopropanoic acid and acetoacetic acid.

In this series of β-keto carboxylic acids, $XCOCH_2COOH$, we have chosen to include malonic acid (containing the electron-withdrawing group, X = OH) and acetoacetic acid (containing a weak electron-donating group, X = CH_3) to compare with 3-oxoproponoic acid (X = H) in order to investigate the substituent influence on the activation energies of the decarboxylations. The hydroxyl group in malonic acid withdraws electron density from the carbonyl carbon resulting in a decrease

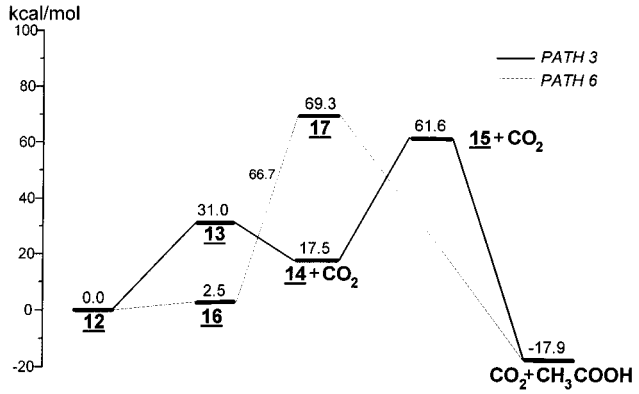

Figure 4. Energy profile for the unimolecular pyrolysis of malonic acid (MP2/6-31G*//MP2/6-31G*).

TABLE 2: Comparison of the Experimental and Theoretical Activation Energies for Malonic Acid

		kcal/mol	solvent
theory	this work	28.5	gas phase
	this work	32.1	$\epsilon = 4.22$
	this work	32.6	$\epsilon = 34.78$
experiment	Hinshelwood	33.0	melt
	Clark	29.0	phenetole
	Clark	28.1	nitrobenzene
	Clark	27.8	β-chlorophentole
	Clark	27.1	*p*-dimethoxybenzene
	Clark	26.9	aniline

TABLE 3: Dipole Moment (debyes)

	1	**2**	**7**	**8**	**12**	**13**
$\epsilon = 1$	4.9	6.4	5.5	6.9	5.2	5.9
$\epsilon = 4.22$	6.2	7.2	6.2	7.2	6.0	6.2
$\epsilon = 34.78$	6.6	7.3	6.6	7.3	6.4	6.4

in the electron density in the neighboring carbonyl group and hence decreases the rate of migration of the carboxyl hydrogen. Therefore, the decarboxylation barrier of malonic acid is found to be higher than that of acetoacetic acid.

3. Solvent Effects. The β-keto carboxylic acids and the corresponding transition structures of their decarboxylations in this study all possess a dipole moment (see Table 3). For the latter these are quite large. The geometries and the relative energies in the gas phase may differ from those in the solution. To assess the influence of solvation on the decarboxylations, the Onsager's reaction field model was applied to (1)−(3) in the media of phenetole (less polar with $\epsilon = 4.22$) and nitrobenzene (polar with $\epsilon = 34.78$). The respective cavity radii are 3.60, 3.65, 3.94, 3.84, 3.67, and 3.72 Å used for structures **1**, **2**, **7**, **8**, **12**, and **13** in the SCRF calculations. It is seen in Figure 1 that the inclusion of a solvent reaction field has only marginal effects on the geometries in (1)−(3) as the calculated SCRF parameters at the HF/6-31G* level are generally close to the corresponding values obtained at the same level in the gas phase. The changes in the bond lengths, bond angles and dihedral angles are −0.074 to 0.276 Å, −1.4 to 3.0°, and −16.9 to 18.0° respectively. It is noteworthy that the polarity of the solvent plays a significant role in bond breaking and formation in the transition structure by lengthening and shortening the respective bonds. This helps to lower activation energy in the decarboxylations.

Similar to the effect on the geometric structures, the solvent effects on the energies are also marginal (see Table 1). A comparison of the energy barriers to decarboxylations in the gas phase and various solvent media shows that in nitrobenzene the magnitudes of the energy lowering (with respect to the gas phase) are 0.7, 0.5, and 0.1 kcal/mol larger than the corresponding values in the less polar medium of phenetole in (1)−(3), respectively, at the HF/6-31G* level (see Table 4). The incorporation of electron correlation further reduces the energy barriers by 10.6−12.7 and 8.4−10.5 kcal/mol at the MP2(Full)/6-31G* // MP2(Full)/6-31G* (the gas phase) and MP2(Full)/6-31G* // HF/6-31G* (in the media) levels of theory, respectively. These trends in barrier lowering as a function of the polarity of solvent at the HF/6-31G* level do not hold for the results at the MP2(Full)/6-31G* level. This may be attributed to the use of the less accurate HF/6-31G* geometries in the single-point SCRF calculations at the MP2(Full)/6-31G* level. Table 4 also shows that the inclusion of electron correlation is far more significant than that of the reaction field in estimating the energy barriers. The activation energies for the decarboxylations in the media of phenetole and nitrobenzene are predicted to be 27.0 and 26.7, 25.2 and 24.8, and 32.1 and 32.6 kcal/mol for (1), (2), and (3), respectively. The latter values for malonic acid in (3) are in good agreement with the corresponding experimental data reported for various media in the literature (see Table 2).

TABLE 4: Relative Activation Energies

	HF[a]			MP2[b]		
	$\epsilon = 1.00$	$\epsilon = 4.22$	$\epsilon = 34.78$	$\epsilon = 1.00$	$\epsilon = 4.22$	$\epsilon = 34.78$
H	39.0	−1.5	−2.2	−12.7	−10.5	−10.2
CH_3	36.8	−1.6	−2.1	−11.1	−10.0	−9.8
OH	41.6	−0.5	−0.6	−10.6	−9.0	−8.4

[a] Relative activation energy to that of $\epsilon = 1.00$. [b] Relative activation energy to that of the HF level.

4. TST Rate Constant Calculations. In order to obtain further information about the thermal decomposition of the β-keto carboxylic acids, the simple transition state theory (TST) was applied to estimate the rate constants (k) of the unimolecular processes from the equation

$$k = \frac{k_B T}{h} \frac{Q^{\ddagger}}{Q_r} e^{-E_a/RT} \qquad (7)$$

where k_B is the Boltzmann constant, T is the temperature in the Kelvin scale, and h is the Planck constant. The respective partition functions $Q^{\ddagger}$ and Q_r for the transition structures and reactants were obtained from the ab initio harmonic frequency calculations at MP2(Full)/6-31G* level. The barrier heights, E_a, were taken from the best estimate of the MP4SDTQ(FC)/6-311++G** single-point calculation based on the MP2(Full)/6-31G** geometries. The vibrational frequencies used in computing the partition functions were not scaled, since the systematic errors from the unscaled harmonic vibrational frequencies tend to be offset in (7).[39] For the same reason the internal rotations were not incorporated. The computations of the TST rate constants were performed using the ART[40] program.

Plots of the resulting frequency factors and rate constants dependencies of temperatures for the thermal decomposition are displayed in Figures 5 and 6, respectively. The activation energies are virtually independent of the temperatures in the range 200−1000 K with the variations being less than 1 kcal/mol, while for the same temperature range, the frequency factor increases from 2.08×10^{12} to 3.75×10^{12}, 3.22×10^{12} to 7.62×10^{12}, and 8.18×10^{12} to 1.54×10^{13}, respectively for X = H, OH, and CH_3 (Figure 6). Finally as can be seen in Figure 6, the computed TST rate constants for the three β-keto carboxylic acids remain nearly the same at the temperatures below 700 K. Temperature dependencies of the rate constants are clearly shown for the thermal decomposition of acetoacetic

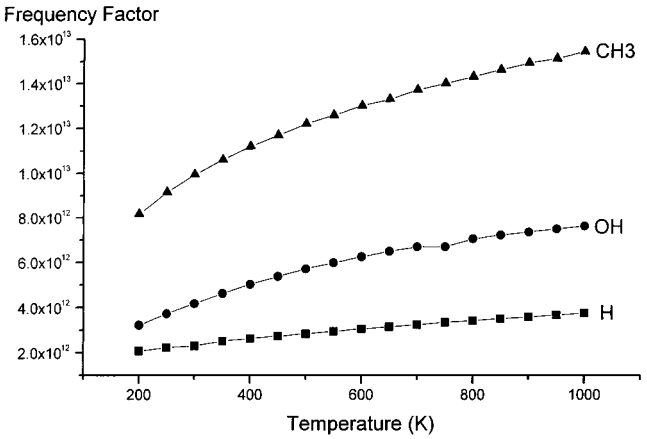

Figure 5. Plot of frequency factors vs temperature.

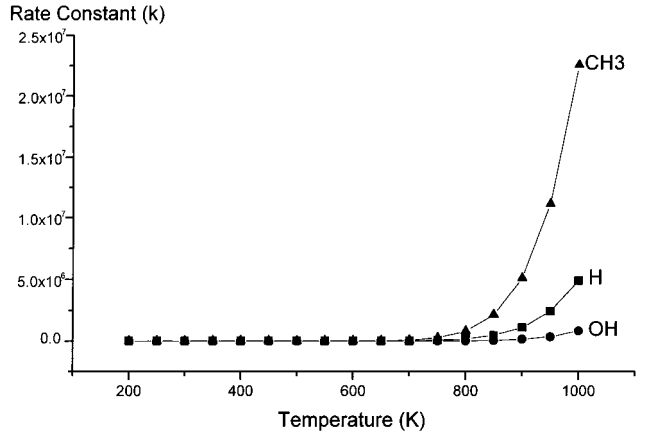

Figure 6. Plot of rate constant vs temperature.

acid (X = CH_3) and 3-oxopropanoic acid (X = H), particularly the former, over the temperature range 800−1000 K. It is interesting to note that the rate of decarboxylation of malonic acid (X = OH) increases only slightly with increasing temperature.

Conclusions

We have examined the decarboxylations of the β-carboxylic acids, $XCOCH_2COOH$ (X = H, CH_3, and OH), using ab initio molecular orbital methods at the HF/6-31G* and MP2(Full)/6-31G* levels of theory. The results from this study predict the reaction pathways of six-membered ring transition structures to be the minimum energy paths. Based on this most likely mechanism, the following conclusions emerge from the present investigation:

(1) Throughout the process of 1,5 shift, the migrating hydrogen carries more than 0.5 positive charge. This indicates a proton-transfer process in the decarboxylation of the β-keto carboxylic acids.

(2) The barriers to decarboxylations in the media of phenetole and nitrobenzene (in parentheses) are predicted to be 27.0 (26.7), 25.2 (24.9), and 32.1 (32.6) kcal/mol for 3-oxopropanoic acid, acetoacetic acid, and malonic acid, respectively. The latter values of malonic acid are in good agreement with the experimental results in liquid phase and solutions (Table 2). The above-calculated data also show that the polarity of a solvent has little effect on the energy barriers.

(3) The calculated rate constants for the decarboxylations of the β-carboxylic acids based on TST deviate at temperatures above 700 K. The deviation becomes more significant as the temperature increases.

Acknowledgment. The authors are grateful to the National Science Council of the Republic of China for continuing financial support and the National Center for High-Performance Computing and the computer center of National Chung-Hsing University for their generous allocation of computing time. They express their appreciation to Professor William L. Hase of Wayne State University for providing the ART program used in the TST calculations.

Supporting Information Available: Tables of geometry structures of all stationary points including SCRF calculations (in Cartesian coordinate), the bond orders, and the population analysis (9 pages). Ordering information is give on any current masthead page.

References and Notes

(1) Blake, P. G.; Davies, H. H.; Jackson, G. E. *J. Chem. Soc. B* **1971**, 1923.
(2) Ruelle, P.; Kesselring, U. W.; Nam-Tran, Hô *J. Am. Chem. Soc.* **1986**, *108*, 371−375.
(3) Ruelle, P. *J. Am. Chem. Soc.* **1987**, *109*, 1722−1725.
(4) Francisco, J. S. *J. Chem. Phys.* **1992**, *96*, 1167−1175.
(5) Goddard, J. D.; Yamaguchi, Y.; Schaefer III, H. F. *J. Chem. Phys.* **1992**, *96*, 1158−1166.
(6) Bamford, C. H.; Dewar, M. J. S. *J. Chem. Soc.* **1949**, 2877.
(7) Blake, P. G.; Jackson, G. E. *J. Chem. Soc. B* **1968**, 1153.
(8) Blake, P. G.; Jackson, G. E. *J. Chem. Soc. B* **1969**, 94.
(9) Mackie, J. C.; Doolan, K. R. *Int. J. Chem. Kinet.* **1984**, *16*, 525−541.
(10) Duan, X.; Page, M. *J. Am. Chem. Soc.* **1995**, *117*, 5114−5119.
(11) Nguyen, M. T.; Sengupta, D.; Raspoet, G.; Vanquickenborne, L. G. *J. Phys. Chem.* **1995**, *99*, 11883−11888.
(12) Back, R. A.; Yamamoto, S. *Can. J. Chem.* **1985**, *63*, 542.
(13) Bock, C. W.; Redington, R. L. *J. Phys. Chem.* **1988**, *92*, 1178−1187.
(14) Back, R. A.; Yamamoto, S. *Can. J. Chem.* **1985**, *63*, 549.
(15) Saito, K.; Sasaki, G.; Okada, K.; Tanaka, S. *J. Phys. Chem.* **1994**, *98*, 3756−3761.
(16) Norris, K. E.; Bacskay, G. B.; Gready, J. E. *J. Comp. Chem.* **1993**, *14*, 699−714.
(17) Lapidus, G.; Barton, D.; Yankwich, P. E. *J. Phys. Chem.* **1964**, *68*, 1863−1865.
(18) Bock, C. W.; Redington, R. L. *J. Chem. Phys.* **1986**, *85*, 5391−5400.
(19) Pollak. *Hofmeisters Beiträge* **1907**, *10*, 234.
(20) (a) Engfeldt. *Beiträge zur Kenntnis der Biochemie der Acetonkörper.* Dissertation, Lund, Sweden, 1920. (b) Widmark, *Acta Med. Scand.* **1920**, *53*, 393; *Skand. Arch. Physiol.* **1922**, *42*, 43. (c) Euler, H. V. *Z. Anorg. Chem.* **1925**, *147*, 295. (d) Wiig, E. O. *J. Phys. Chem.* **1928**, *32*, 961.
(21) Ljunggren. *Katalytisk Kolsyreavspjälkning ur Ketokarbonsyror.* Dissertation, Lund, Sweden, 1925.
(22) Pedersen, K. J. *J. Am. Chem. Soc.* **1929**, *51*, 2098.
(23) Swain, C. G.; Bader, R. F. W.; Esteve, R. M.; Griffin, R. N. *J. Am. Chem. Soc.* **1961**, *83*, 1951−1955.
(24) Bigley, D. B.; Thurman, J. C. *Tetrahedron Lett.* **1967**, *25*, 2377.
(25) Westheimer, F. H.; Jones, W. A. *J. Am. Chem. Soc.* **1941**, *63*, 3283.
(26) Esteve, R. M. Jr. *Ph.D. Thesis in organic Chemistry*, M.I.T., December 1950; pp 34−126.
(27) Bigley, D. B.; and Thurman, J. C. *J. Chem. Soc. B* **1968**, 436.
(28) (a) Hinshelwood, C. N. *J. Chem. Soc.* **1920**, *117*, 156. (b) Clark, L. W. *J. Phys. Chem.* **1961**, *65*, 2271. (c) Clark, L. W. *IBID.* **1958**, *62*, 368. (d) Clark, L. W. *IBID.* **1958**, *62*, 79. (e) Clark, L. W. *J. Chem. Soc.* **1962**, *66*, 125.
(29) Frisch, M. J.; Trucks, G. W.; Head-Gordon, M.; Gill, P. M. W.; Wong, M. W.; Foresman, J. B.; Johnson, B. G.; Schlegel, H. B.; Robb, M. A.; Replogle, E. S.; Gomperts, R.; Andres, J. L.; Raghavachari, K.; Binkley, J. S.; Gonzalez, C.; Martin, R. L.; Fox, D. J.; Defrees, D. J.; Baker, J.; Stewart, J. J. P.; Pople, J. A. *Gaussian 92*, Revision C.4; Gaussian, Inc.: Pittsburgh, PA, 1992.
(30) (a) Moller, C.; Plesset, M. S. *Phys. Rev.* **1934**, *46*, 618. (b) Pople, J. A.; Binkley, J. S.; Seeger, R. *Int. J. Quantum Chem., Symp.* **1976**, *10*, 1. (c) Krishnan, R.; Pople, J. A. *Int. J. Quantum Chem.* **1978**, *14*, 91.
(31) (a) Hariharan, P. C.; Pople, J. A. *Theor. Chem. Acta.* **1973**, *28*, 213. (b) Francl, M. M.; Pietro, W. J.; Hehre, W. J.; Binkley, J. S.; Gordon, M. S.; Pople, J. A. *J. Chem. Phys.* **1982**, *77*, 3654.

(32) Pople, J. A.; Luke, B. T.; Frisch, M. J.; Binkley, J. S. *J. Phys. Chem*. **1985**, *89*, 2198−2203.
(33) Wong, M. W.; Wiberg, K. B.; Frisch, M. J. *J. Am. Chem. Soc.* **1992**, *114*, 1645−1652.
(34) (a) NBO Version 3.1; Glendening, E. D.; Reed, A. E.; Carpenter, J. E.; Weinhold, F. (b) Foster, J. P.; Weinhold, F. *J. Am. Chem. Soc*. **1980**, *102*, 7211. (c) Reed, A. E.; Weinhold, F. *J. Chem. Phys*. **1983**, *78*, 4006. (d) Reed, A. E.; Weinstock, R. B.; Weinhold, F. *J. Chem. Phys*. **1985**, *83*, 735. (e) Carpenter, J. E.; Weinhold, F. *J. Mol. Struct*. **1988**, *169*, 41. (f) Reed, A. E.; Curtiss, L. A.; Weinhold, F. *Chem. Rev*. **1988**, *88*, 899.
(35) Gonzalez, C.; Schlegel, H. B. *J. Chem. Phys*. **1989**, *90*, 2154.
(36) (a) Onsager, L. *J. Am. Chem. Soc.* **1936**, *58*, 1486. (b) Tapia, O.; Goscinski, O. *Mol. Phys*. **1975**, *29*, 1653. (c) Wong, M. W.; Frisch, M. J.; Wiberg, K. B. *J. Am. Chem. Soc*. **1990**, *112*, 4776.
(37) Burn, P.; Weagell, B. In *Reactive Intermediates*; Plenum: New York, 1983; Vol. 3, p 367 and references therein.
(38) (a) Schenkel, H.; Klein, A. *Helv. Chim. Acta* **1945**, *28*, 1211. (b) Cantwell, N. H.; Brown, E. V. *J. Am. Chem. Soc.* **1953**, *117*, 156.
(39) Heuts, J. P. A.; Gilbert, R. G.; Radom, L. *J. Phys. Chem.* **1996**, *100*, 18997−19006.
(40) ART was obtained from Professor William L. Hase of Wayne State University.